Journal of Hazardous Materials 162 (2009) 222–229

Contents lists available at ScienceDirect

Journal of Hazardous Materials

journal homepage: www.elsevier.com/locate/jhazmat

Directed site exploration for permeable reactive barrier design

Jejung Lee[a,*], Andrew J. Graettinger[b], John Moylan[c], Howard W. Reeves[d]

[a] Department of Geosciences, University of Missouri-Kansas City, Kansas City, MO 64110, United States
[b] Department of Civil and Environmental Engineering, University of Alabama, Box 870205 Tuscaloosa, AL 35487, United States
[c] 5306 W.57th Street, Shawnee Mission, KS 66205, United States
[d] U.S. Geological Survey, USGS Michigan Water Science Center, 6250 Mercantile Way, Suite 5, Lansing, MI 48911, United States

ARTICLE INFO

Article history:
Received 26 December 2007
Received in revised form 4 May 2008
Accepted 6 May 2008
Available online 13 May 2008

Keywords:
Permeable reactive barrier
Site exploration
Uncertainty analysis

ABSTRACT

Permeable reactive barriers (PRBs) are being employed for in situ site remediation of groundwater that is typically flowing under natural gradients. Site characterization is of critical importance to the success of a PRB. A design-specific site exploration approach called quantitatively directed exploration (QDE) is presented. The QDE approach employs three spatially related matrices: (1) covariance of input parameters, (2) sensitivity of model outputs, and (3) covariance of model outputs to identify the most important location to explore based on a specific design. Sampling at the location that most reduces overall site uncertainty produces a higher probability of success of a particular design. The QDE approach is demonstrated on the Kansas City Plant, Kansas City, MO, a case study where a PRB was installed and failed. It is shown that additional quantitatively directed site exploration during the design phase could have prevented the remedial failure that was caused by missing a geologic body having high hydraulic conductivity at the south end of the barrier. The most contributing input parameter approach using head uncertainty clearly indicated where the next sampling should be made toward the high hydraulic conductivity zone. This case study demonstrates the need to include the specific design as well as site characterization uncertainty when choosing the sampling locations.

1. Introduction

Permeable reactive barriers (PRBs) are being employed as an in situ treatment technology for groundwater contamination. A PRB is designed to intercept a plume of contaminated groundwater moving under the natural gradient and transform the contaminant into an environmentally acceptable form. The goal is to have contaminant levels below target concentration at compliance points down gradient of the barrier. The barrier is made out of a reactive media that is selected based on the type of contaminant. The most common form of reactive media is zero-valent iron (Fe^0). When, for example, chlorinated organics come in contact with Fe^0, they are potentially degraded into nontoxic dehalogenated organic compounds and inorganic chloride [1]. The ability of a PRB to dehalogenate a compound is a significant benefit, especially for a plume of dense non-aqueous phase liquid (DNAPL). This is because the residuals of a DNAPL contamination cannot be easily located and may continue to generate a plume of dissolved hydrocarbons [2]. Although the pump and treat (PT) technique can control such a DNAPL plume, PT requires extensive long-term maintenance and continual energy input. In contrast, a DNAPL plume can be controlled with a PRB with minimal maintenance because PRBs operate in a totally passive manner. Other advantages of PRBs are: (1) contaminants are treated away from the surface, which minimizes worker and public exposure to toxic contaminants and (2) waste constituents are concentrated into a relatively small volume within the treatment zone, which is the barrier itself.

There are several disadvantages of using PRBs though. First, long-term performance of PRBs may generate preferential flows through the barrier with pore clogging, thus the PRB itself becomes heterogeneous and ineffective for treatment [3]. Second, hydraulic heterogeneity of the subsurface around the barrier can cause so much uncertainty in performance that use of a passive PRB is precluded [4]. Schipper et al. [5] investigated the effect of hydraulic conductivity change during the construction of denitrification wall and found that the performance of permeable wall approaches was highly dependent on the aquifer material. Gupta and Fox [6] implemented groundwater flow modeling and particle tracking techniques to find how aquifer heterogeneity affects the performance of PRB for different design parameters such as the capture zone width, residence time, flow velocity, and discharge.

US Environmental Protection Agency (EPA) [7] reported the use of PRBs for contaminated groundwater treatment at 47 sites in

* Corresponding author. Tel.: +1 816 235 6495; fax: +1 816 235 5535.
E-mail addresses: leej@umkc.edu (J. Lee), andrewg@eng.ua.edu (A.J. Graettinger), john_moylan@sbcglobal.net (J. Moylan), hwreeves@usgs.gov (H.W. Reeves).

0304-3894/$ – see front matter © 2008 Elsevier B.V. All rights reserved.
doi:10.1016/j.jhazmat.2008.05.026

the United States, Canada, and selected locations abroad. One of the lessons learned from this study was the importance of extensive site characterization during the design phase, which is the period when the remedial design parameters are determined and the best remedial option is selected. Two cases were presented in the EPA report, The Kansas City Plant (KCP) case and the Fry Canyon case, which demonstrate how insufficient site characterization affected the performance of the PRBs. At the KCP site a continuous trench PRB was designed and installed to treat 1,2-dichloroethylene (1,2-DCE) and vinyl chloride (VC). It was found during operation that a high concentration of contaminants was passing around the end of the barrier due to a high conductive zone, which was not detected during the design site exploration phase. The Fry Canyon site adopted a funnel-and-gate design to treat uranium contamination in groundwater. Although the design had funnels—no flow barriers to block the bypass of contaminants, the incomplete contact between the uneven surface of the underlying confining unit and the gates provided pathways for contaminated groundwater. In addition, a large bedrock nose was detected during the PRB installation and resulted in re-orientation of the PRB with an oblique angle into the funnels. Therefore, the design should be site-specific with a thorough understanding of subsurface heterogeneity.

It is suggested that a design phase of site exploration be employed to select an appropriate remediation technique, which is then followed by a design-specific site exploration. Additional site exploration is usually not considered after the remedial design is chosen. Case studies indicate that if additional site exploration had been performed with a specific design in mind, many cases of remedial failure could have been avoided. It should be noted that the additional site exploration should be design-specific so that the additional information can be used to optimize the design parameters to avoid potential failure.

Four aspects of site characterization that should be evaluated before implementing a PRB are: (1) hydrogeology, (2) contaminant loading, (3) geochemistry, and (4) microbiology [8]. Hydrogeologic characterization must be done accurately as it determines groundwater flow patterns and the distribution of the contaminant plume. Inaccurate flow patterns may cause bypass of contaminant around the barrier and lead to a potential failure of remediation. It is also necessary to have an adequate contaminant characterization (such as maximum concentration) and total mass of contaminant as these parameters determine the dimensions of the PRB. Geochemical characterization is needed for estimating the expected life of a PRB system because, for example, the potential effect of precipitation buildup on the medium may cause bypassing of the barrier. The microbial aspects of the PRB should be known as well since the interactions of native microbial populations, contaminants, and reactive barrier materials are quite complex.

It is well documented in the literature that hydrogeologic site characterization is critical to the success of a PRB, yet there are relatively few studies emphasizing site characterization for PRBs. Most PRB studies focus on the determination of PRB design parameters such as length, thickness, angle, or hydraulic conductivity of the barrier and simply employ a groundwater flow model to assist in the design parameter determination (for example, Scott and Folkes [9]). Although not the primary focus of a paper, some research has been published on the uncertainty of site conditions associated with PRBs' design parameters [10]. Heterogeneity of the hydrogeologic settings and its effect on the performance of PRBs has been secondarily considered [11,12]. Typically a stochastic approach using a Monte Carlo simulation is employed to propagate hydrogeologic uncertainty through a model to the result. Accounting for uncertainty is critical to the success of a PRB, but additional directed site exploration to reduce the uncertainty in site conditions prove a more economical and conservative approach rather than over-designing caused by a lack of data.

Unlike current published literature, the present study focuses on additional site exploration after a specific design has been selected. The present approach may reduce the uncertainty in site conditions and find potentially hidden hydrogeologic structures that may adversely affect the performance of a PRB. Published site exploration studies for hydrologic conditions generally focus on model calibration [13–16]. The unknown or inaccurate parameters are calibrated by minimizing the differences between observed data and model outputs—typically head elevation and concentration. Methods exist to improve model calibration through directed exploration that employs a number of techniques including: prediction sensitivity and kriged error variance [17,18], minimizing model prediction uncertainty [15], composite scaled sensitivities [19], and value of improved information [20]. Cirpka et al. [21] employed a first-order second moment (FOSM) method to determine whether the funnel-and-gate system would succeed or fail by tracing variance reduction in the streamline functions. The position of most data worth for the variance reduction becomes an additional sampling location, so that the reliability of decision for the design success or failure increases. The quantitatively directed exploration (QDE) approach presented herein is very close to the study of Cirpka et al. [21] in a sense of directed sampling using uncertainty. The difference is that instead of using the PRB performance, we identify which input data have the greatest effect on model results given a specific design by rearranging matrix calculation in FOSM and find the data location that contributes the most to output variances across a site for a given PRB design. The original concept for QDE was to direct exploration to the location of greatest variance in model outputs, which is where model results are most uncertain [22–24]. This QDE approach has been successfully applied to groundwater remediation to find a next sampling location that is most likely to increase remedial design reliability [22]. Further development of the QDE approach by Graettinger et al. [23] investigated and evaluated seven different techniques to direct exploration through re-analysis and comparison of the input variance matrix, output variance matrix, and model sensitivity matrix using MODFLOW 2000 [16]. This work determined that the piezometric head model was most improved by obtaining additional samples at locations where input information contributed the most to overall output variance. Lee [22] showed how directed exploration increased design reliability as compared to random sampling for a PT method. Additional QDE sampling of transmissivity reduced the uncertainty of predicted concentration while the sensitivity of predicted concentration to transmissivity did not significantly change.

In the study presented herein, we adopted the QDE approach to demonstrate how additional exploration produces a higher probability of success of a particular PRB design. We used the KCP case study to show how QDE is able to detect unrevealed site conditions that may affect the performance of PRBs.

2. Methodology

All QDE approaches in Graettinger et al. [23] are based on three matrices: (1) covariance of input parameters, (2) sensitivity of model outputs, and (3) covariance of model outputs. Each of the data elements in these matrices is related to a specific location within a site. Therefore a precise parameter and location can be identified for additional sampling. Each of these matrices, input covariance, model sensitivity, and output covariance, are described in detail in this section.

2.1. Input parameter estimation and covariance

The QDE approach uses a multivariate normally distributed conditional probability calculation to interpolate and extrapolate input parameters. This calculation generates a regularized grid of input data values and associated spatially distributed uncertainty (covariance) that is assumed to be normally distributed about the mean value of the input data at each finite difference grid location. For the KCP case study presented, hydraulic conductivity is the uncertain spatially distributed input parameter. During estimation of hydraulic conductivity, the measured hydraulic conductivities at sampled locations are stored in a vector, $\boldsymbol{V}$. Next, a vector, $E(\boldsymbol{U})$, is produced that contains a prior estimate of mean hydraulic conductivity at each grid point. Finally an informed prior covariance matrix, Cov($\boldsymbol{U}$), is calculated by employing a variogram function that represents the covariance relationships between the known hydraulic conductivities at sampled locations. From these matrices, the prior estimates, $E(\boldsymbol{U})$ and Cov($\boldsymbol{U}$), are updated to posteriors, $E(\boldsymbol{U}|\boldsymbol{V})$ and Cov($\boldsymbol{U}|\boldsymbol{V}$), using data from the sampled points, through the following equations [25]:

$$E(U|V) = E(U) + \mathrm{Cov}(U, V)\mathrm{Cov}(V)^{-1}(V - E(V)) \quad (1)$$

$$\mathrm{Cov}(U|V) = \mathrm{Cov}(U) - \mathrm{Cov}(U, V)\mathrm{Cov}(V)^{-1}\mathrm{Cov}(V, U) \quad (2)$$

$E(\boldsymbol{U}|\boldsymbol{V})$ is the updated vector of hydraulic conductivities given the known hydraulic conductivities at the sampled locations. Cov($\boldsymbol{U}$, $\boldsymbol{V}$) is a subset of the full covariance matrix that stores the covariance between the hydraulic conductivities being estimated and the known hydraulic conductivities at sampled locations. Cov($\boldsymbol{V}$)$^{-1}$ is again a subset of the full covariance matrix, and is the inverse of the covariance between the known hydraulic conductivities. $E(\boldsymbol{V})$ is a subset of $E(\boldsymbol{U})$ and holds the prior hydraulic conductivities estimates at the sampled locations. Cov($\boldsymbol{U}|\boldsymbol{V}$) is the updated covariance matrix, and Cov($\boldsymbol{U}$) is the prior covariance matrix, calculated by the covariance function. A FORTRAN program was written to estimate the hydraulic conductivity data and its associated uncertainty using conditional probability calculations shown in Eqs. (1) and (2). Generated output files were then used as input for groundwater flow and contaminant transport models.

2.2. Model sensitivity

The sensitivity matrix was calculated by the DDC method [22,26]. In the DDC method, derivatives of dependent variables are coded directly in to the original program, which then simultaneously produces model outputs and derivatives of those outputs. The DDC method is based on the chain rule of differentiation. The DDC differentiates all variables related to dependent variables such as head and/or concentration in a sequential manner. Programming of the derivatives was accomplished by hand coding and by employing ADIFOR 2.0 [27], which is an automated derivative coding program. In our case study, a flow model and a transport model are independent simulators, so the derivatives of head and concentration were produced independently by ADIFOR 2.0, and then linked by the derivatives of Darcian velocities, which were programmed manually. Details of the DDC process are described in Lee [22].

2.3. First-order second moment (FOSM) calculation

Within the QDE framework, input parameter covariance and model sensitivity are combined through a first-order Taylor series expansion to produce the variance in computed output. For example, calculation of piezometric head covariance from correlated hydraulic conductivities is shown by Eq. (3) [28].

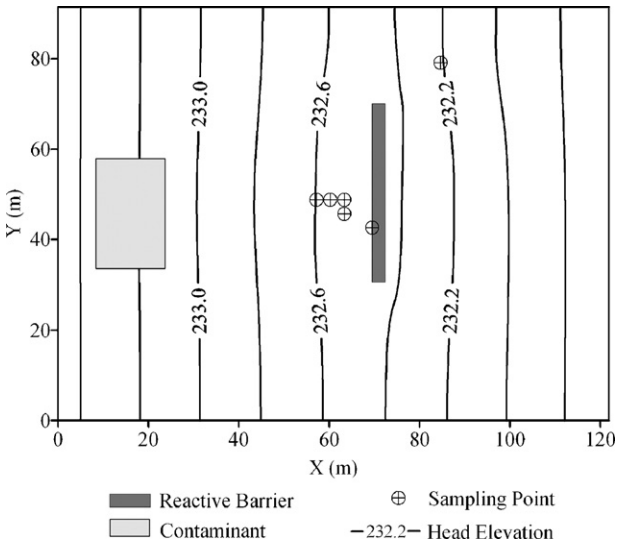

Fig. 1. Plan view of groundwater flow and initial plume geometry including six initial sample borings and the reactive barrier. The maximum concentration of the plume is 2000 μg/L for 1,2-DCE and the head elevations are constant at both the east and west ends of the site. The unit of head elevation is m.

Table 1
Hydraulic conductivities at the six initial sample locations

Well no.	X (m)	Y (m)	Hydraulic conductivities (m/day)
1	54.9	48.8	10.4
2	57.9	48.8	9.8
3	61.0	48.8	9.1
4	61.0	45.7	9.1
5	67.1	42.7	8.2
6	82.3	79.3	3.4

$$\mathrm{Cov}[h_l, h_k] \approx \sum_{i=1}^{n}\sum_{j=1}^{n}\left(\frac{\partial h_l}{\partial \bar{K}_i}\right)\left(\frac{\partial h_k}{\partial \bar{K}_j}\right)\mathrm{Cov}[K_i, K_j] \quad (3)$$

Here Cov[h_l, h_k] is the covariance of computed head (h) between node l and node k. $(\partial h_k/\partial \bar{K}_i)$ is the sensitivity of head at node k to a change in the hydraulic conductivity (K) at node i. Cov[K_i, K_j] is the covariance between hydraulic conductivities at nodes i and j.

Using the input parameter and covariance files produced by Eqs. (1) and (2), and the sensitivity matrix from the direct derivative coding (DDC) calculation, covariances in predicted piezometric head and concentration are calculated for the entire model using Eq. (3).

Table 2
Input parameters used to model the KCP site

	Values
Hydraulic parameters	
Longitudinal dispersivity (a_L)	0.6 m
Transverse dispersivity (a_T)	0.3 m
Diffusion coefficient	4.7×10^{-4} m^2/day
Storativity	0.001
Porosity	0.33
Numerical parameters	
Area size	121.9 m × 91.4 m
Element size (triangular)	3 m × 3 m
Total number of nodes	1271
Total number of elements	1200
Size of time step	10 days
Total simulation time	100 days

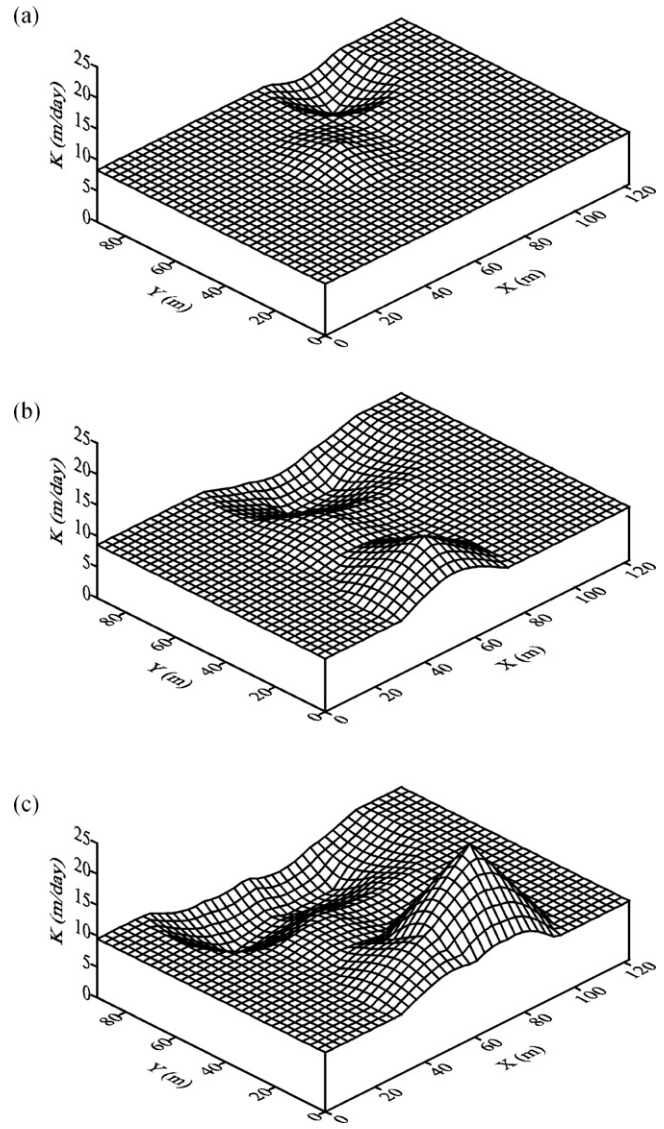

Fig. 2. Updating hydraulic conductivity (K) distribution using MCI for head. (a) K surface map from the initial six samples, (b) K surface map from the eight samples, and (c) K surface map from the ten samples.

The use of the FOSM method to find a next sampling location has limitations. First, the derivatives are calculated at the expected value of the input parameter; therefore, if there is a large uncertainty associated with the parameter then the derivative may not be equal to the true derivative [28]. Second, input parameters are assumed to be statistically independent of each other. Finally, the FOSM method requires knowledge of the uncertainty associated with each input parameter, which in this example is produced from a conditional probability calculation based on the variogram model.

2.4. QDE approaches

Among seven approaches presented in Graettinger et al. [23], two approaches, the largest variance (LV) and most contributing input (MCI) to output covariance were applied in this PRB example. The LV identifies the location of the largest output uncertainty produced from input parameters. This is the original QDE approach proposed by Graettinger and Dowding [26] and Lee [22] that directs exploration to the next sampling location where the output variance is the largest. The output variances are the diagonal elements of Cov[h_l, h_k] in Eq. (3). Although a variance in a model domain is related to a single cell at a site, its calculation is the sum of input parameter covariance and model sensitivity from across a site, not the single cell only. A situation can arise where the location of greatest output variance has already been sampled. In this case, the input variance at that location is zero with the assumption of zero measurement error, but that location still has the maximum uncertainty because the output variance is a sum of information from across a site. Re-sampling at that location adds no new information to the analysis; therefore, the LV must identify the location of maximum output variance that has not been previously sampled.

The MCI approach to direct exploration chooses the location where input parameter uncertainty contributes the most to output uncertainty. As discussed with the LV, it is possible to have the maximum output variance at a location that has been previously sampled. Re-sampling at that location will not improve the model or reduce uncertainty. The FOSM equation, Eq. (3), is re-arranged to sum output variance terms related to an input parameter at a specific location. Eq. (4) represents the contribution of a parameter at ith location to the output variances across a site having n model cells or nodes.

$$\mathrm{cont}(i) = \sum_{j=1}^{n} \left\{ \sum_{k=1}^{n} \left(\frac{\partial h_j}{\partial K_i} \right) \mathrm{Cov}(K_i, K_k) \left(\frac{\partial h_j}{\partial K_k} \right) \right\} \quad (4)$$

Here, cont(i) is the contribution to output variance from an input parameter, K_i, that is correlated with other parameters. By comparing cont(i) from $i = 1$ to n for a given model, the maximum cont(i) is the location of the input parameter that contributes the most to total output covariance.

In the present study, we use the MCI approach to choose the location of largest cont(i) as the next sampling location and find how that additional measurement improves the PRB performance. We also compare LV and MCI for head uncertainty and concentration uncertainty to show which approach is the best at reducing uncertainty associated with a PRB design.

3. Case study—Kansas City Plant, Kansas City, MO

In 1942 the Kansas City Plant (KCP) was built to produce aircraft engines during World War II and later non-nuclear components of nuclear weapons. The plant is located on the south side of downtown Kansas City, MO. Presently, the KCP's primary mission is to produce and procure non-nuclear electric, electronic, mechanical, plastic, electromechanical, and non-fissionable metal components for the Department of Energy's (DOE's) weapons program. Spills and accidental leaks from long time military production activities resulted in soil and groundwater contamination.

A groundwater plume emanates from the northeast area of the plant. Volatile organic compounds (VOCs) including trichloroethylene (TCE), 1,2-DCE and vinyl chloride are the major components within the plume, which was more than 61 m wide in the vicinity of the PRB. The immediate concern was VOC contamination of the Blue River, a tributary of the Missouri River. A meander loop of the Blue River was bypassed as part of a flood control

Table 3
Additional sampling locations and measured hydraulic conductivities

Approach	Updating	X (m)	Y (m)	Hydraulic conductivities (m/day)
MCI for head	1st	64.0	79.2	0.9
		51.8	12.2	15.5
	2nd	39.6	76.2	2.4
		76.2	18.3	24.4

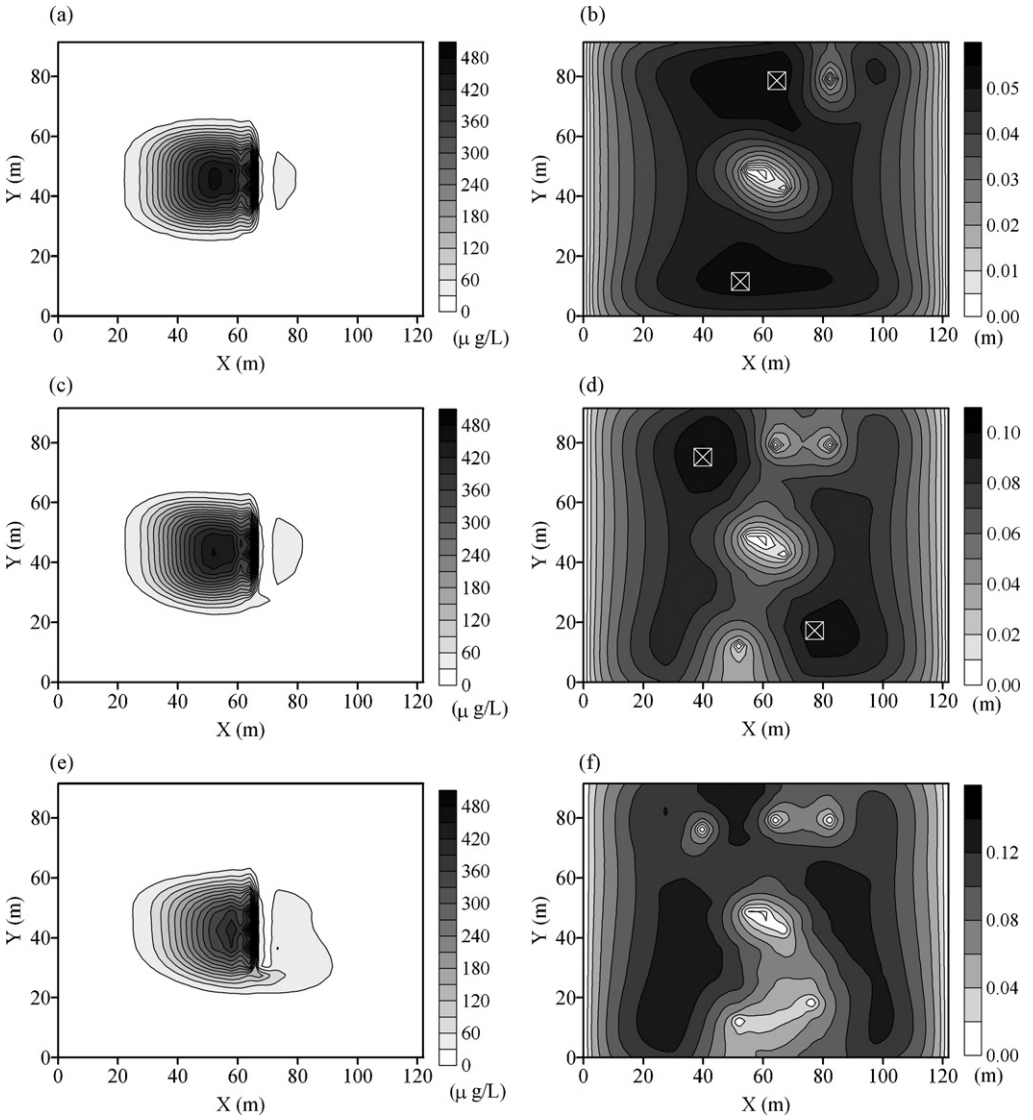

Fig. 3. Predicted concentration distributions and MCI maps. (a) Concentration and (b) MCI from the initial six samples. (c) Concentration and (d) MCI from eight samples. (e) Concentration and (f) MCI from ten samples. The white crossed boxes indicate the next sampling location having the highest MCI values.

initiative in the early 1960s. The existence of the old river structure makes a complex hydrologic and geologic condition in this area. Basically, an upper clayey-silt layer is underlain by a basal gravel layer throughout the site. The thickness of each layer is non-uniform and sometimes disconnected. According to the slug and pumping test results in DOE [29], the hydraulic conductivities in each layer are highly varied; 0.3–61 m/day with an average of 10 m/day for the basal gravel layer and 0.03–12 m/day with an average of 0.23 m/day for the upper clayey-silt layer. The water levels in the more permeable basal gravel layer were 0.3–0.6 m lower than the water levels in the less permeable clayey-silt, thus creating a downward hydraulic gradient.

To prevent the transport of contaminant to the Blue River, an interceptor trench was dug, which contained the plume from 1990 until 1998. The PRB was installed to replace the interceptor trench in 1998. Although this passive iron wall treated 97 percent of the contaminant mass, the performance and monitoring results showed that the contaminants were not being sufficiently degraded near the southern end of the wall and bypass of the southern end of the wall was occurring [29]. One explanation for the bypass was that the basal gravel layer in the southern quarter of the iron wall had hydraulic conductivities ten times greater than those used during the design of the PRB. If such a high conductive zone had been detected during the design phase of the PRB, bypassing of the PRB could have been avoided.

The present study applies the QDE approach to the KCP site in an attempt to detect the high conductive zone at the south end of the barrier during the design phase. Among the initial set of measurements from the real sampling, we chose six locations around the potential position of the barrier in Fig. 1 by assuming that directed sampling would start from such clustered distribution of sampling. The six measurements of hydraulic conductivity are listed in Table 1. Fig. 1 also shows the two-dimensional finite element model for the study area. The size of the PRB is 67 m wide and 3 m thick with a hydraulic conductivity of 61 m/day. We assumed the decay rate of the iron wall is 0.93/day. Both sides of the site are set as constant head boundaries at 233.5 m for the west side and 231.6 m for the east side. Therefore, the groundwater flows from west to east. The allowable concentration after treatment is 70 μg/L. The uncertain input parameter is hydraulic conductivity, K. Other input parameters and numerical parameters are listed in Table 2.

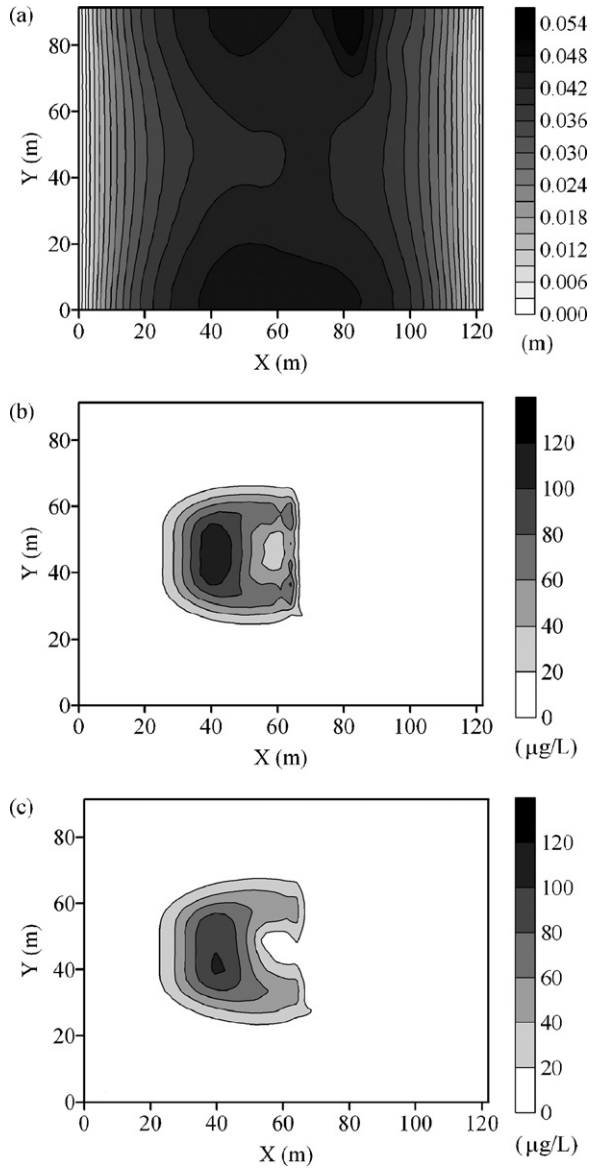

Fig. 4. MCI and LV maps. (a) LV map for head, (b) LV map for concentration, and (c) MCI map for concentration.

Employing the six hydraulic conductivity measurements from the sample locations, the initial hydraulic conductivity distribution for the site is calculated through a multivariate normally distributed conditional probability calculation shown in Eq. (1). Although a constant prior hydraulic conductivity was used across the case study site, a varying or trending prior could be employed. Measured hydraulic conductivities at the six locations are analyzed to estimate their spatial continuity using a variogram function. Since the multivariate conditional calculation employs a variogram, the estimation of variogram parameters such as sill and range is the first step to extrapolate spatial input parameters. The estimates of variogram parameters are, however, performed in a subjective manner. The range, a measure of spatial continuity, influences the smoothness of the input information and uncertainty, while the sill, a measure of the variance in the data set, affects the magnitude of the uncertainty [22,30]. The subjective nature of these estimates may affect the input parameters and associated uncertainty, and therefore, may causes errors in estimating the true output and output uncertainty [31].

For the six measurements, it was determined that the best-fit variogram is a Gaussian function. As the sampling locations are clustered around the barrier, the range is short, only 18.3 m and the sill is 5.57 m^2/day^2. Fig. 2(a) shows the hydraulic conductivity from the six measurements as a surface calculated by Eq. (1). The full covariance matrix from Eq. (2) is multiplied by the full sensitivity matrix using the MCI in Eq. (4).

Fig. 3(a) shows the predicted concentration of the plume after 100 days of transport. Although the figure shows that the barrier can properly treat the plume, we know the plume is uncertain because of uncertain input data. Fig. 3(b) is the MCI map showing the contribution of input parameter (hydraulic conductivity) to the output (head) uncertainty. On this map, dark areas show locations where input uncertainty contributes the most to output uncertainty. The two highest values of cont(i) from Eq. (4) are marked as cross symbols at (X, Y) = (64.0 m, 79.2 m) and (51.8 m, 12.2 m) in Fig. 3(b). At this point the site exploration would be directed to sample the site at the two marked locations. In the present application, the K values at the marked locations were estimated from reported DOE values [29]. The new data are listed in Table 3.

As the two new measured K values are significantly different from other six values that were initially provided, the continuity information within the variogram for hydraulic conductivity should be updated. The updated variogram has a sill of 37.2 m^2/day^2, which is much higher than the previous sill from the original six measurements, and the updated variogram has a longer range of 24.4 m. With the additional sampling at (X, Y) = (51.8 m, 12.2 m), the region having high K around the south end of the barrier is revealed (surface map shown in Fig. 2(b)). Fig. 3(c) shows the modeled plume and Fig. 3(d) shows the MCI map using the K distribution from the eight samples. Compared to Fig. 3(b), Fig. 3(d) shows new locations to sample, marked with a cross symbol.

With the additional two measurements, there is slight bypass of contaminant at the south end of the barrier. Assuming that this slight bypass triggers additional sampling, two more additional measurements should be taken at the marked locations in Fig. 3(d). Their location and K values are listed in Table 3. A variogram analysis was performed and it was found that the two additional measurements in Fig. 3(d) do not significantly change the continuity of hydraulic conductivity. Therefore, the same sill and the range from the previous variogram with eight measurements were used. Fig. 2(e) shows the updated K distribution with ten measurements. The high K distribution with 24.4 m/day is clearly observed at the south end of the barrier while the low K distribution at about 3.0 m/day is observed near the north end of the barrier. The highly varied K distribution around the barrier significantly affects the movement of the plume. Fig. 3(e) shows the bypass of the plume around the south end of the barrier with a concentration that is higher than the allowable concentration. If the bypass is detected with the additional samples during the design phase, the design can be changed by extending the length of the barrier, thus preventing a potential failure due to insufficient site characterization.

A comparison between MCI and LV was performed to find out which of these sampling approaches is most efficient at preventing a potential failure of the PRB by missing an important hydrogeologic structure. The QDE approach can be used to direct exploration based on any model output, which for this case could be head or concentration. We applied MCI and LV to both head uncertainty and concentration uncertainty. Fig. 4 shows the LV maps for head and concentration, and the MCI map for concentration from the initial six measurements. To identify the next sampling locations, the LV map for head in Fig. 4(a) was employed. It shows two regions having similarly high values, thus indicating locations to sample. Regardless of the QDE method, the concentration distribution in Fig. 4(b) and (c) shows

Table 4
Additional sampling locations and measured hydraulic conductivities from MCI and LV for head and concentration

Approach	Updating	X (m)	Y (m)	Hydraulic conductivities (m/day)
LV for head	1st	82.3	85.3	9.1
	2nd	54.9	3.0	15.2
		82.3	76.2	9.1
		57.9	0.0	15.2
MCI for concentration	1st	39.6	48.8	3.0
	2nd	36.6	51.8	2.4
LV for concentration	1st	42.7	45.7	3.0
	2nd	33.5	42.7	2.4

a region of high values, which is behind the barrier. Based on this information, we chose two sampling points from Fig. 4(a) and one sampling point from Fig. 4(b) and (c). The LV map for head in Fig. 4(a) tends to find the southern portion of the barrier, but the next sampling locations are very close to the previously sampled locations. As was done in the previous example, two rounds of exploration were performed and the additional sampling data are listed in Table 4 for each approach.

Fig. 5 shows the *K* and concentration distributions from the three approaches produced from the model using the *K*s listed in Table 4. For directing exploration based on concentration uncertainty, the additional sampling from both the MCI and LV approaches are gathered around the barrier because this directed exploration is highly dependent on the predicted distribution of concentration. The strong dependency on the predicted concentration also causes the dependency on the simulation time as the concentration distribution significantly changes with time. Therefore, the high conductive zone at the south end of the barrier was only revealed by the MCI based on head uncertainty. Fig. 5(b), (d), and (f) shows the predicted concentration at 100 days from three approaches. As expected from

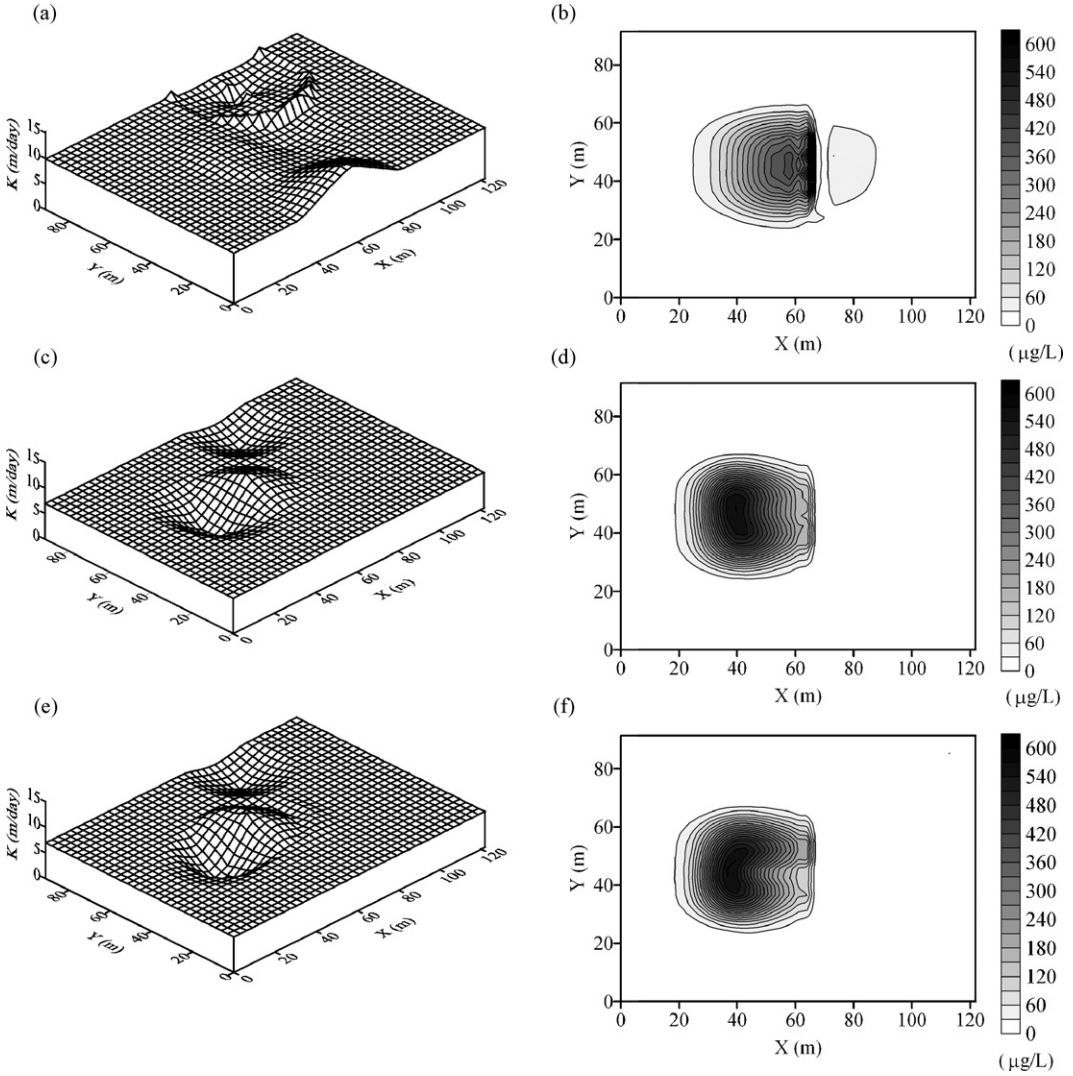

Fig. 5. *K* and predicted concentration distributions. (a) *K* and (b) concentration from LV for head uncertainty using ten samples, (c) *K* and (d) concentration from MCI for concentration uncertainty using eight samples, and (e) *K* and (f) concentration from LV for concentration uncertainty using eight samples.

the K distributions in Fig. 5(a), (c), and (e), only the MCI for head uncertainty revealed the potential bypass of contaminant at the south end of the barrier.

4. Conclusion

A QDE approach using the MCI parameter to output covariance was presented for PRB remediation. As the PRB strongly relies on the groundwater distribution in the subsurface, additional data reducing uncertainty of site conditions and model predictions is considered beneficial. This approach was applied to the Kansas City Plant case and implies that the additional site exploration during the design phase could have prevented the remedial failure that was caused by missing a geologic body having high hydraulic conductivity at the south end of the barrier. The MCI parameter approach clearly indicates where the next sampling should be made to reduce the uncertainty of the model prediction, while the LV approach can direct exploration to a previously sampled location. The comparison between LV and MCI for head uncertainty and concentration uncertainty shows that MCI for head uncertainty was able to find the bypass of contaminant due to the high hydraulic conductivity at the south end of barrier. In order to guarantee the results, more real case studies are required in the future.

Acknowledgement

This work was funded by a Faculty Research Grant from the University of Missouri at Kansas City. We thank anonymous reviewers and the editor handling the manuscript for their constructive remarks. The work has not been subjected to USGS review and, therefore, does not necessarily reflect the views of USGS and no official endorsement should be inferred.

References

[1] A.R. Gavaskar, Design and construction technique for permeable reactive barriers, J. Hazard. Mater. 68 (1999) 41–71.
[2] National Research Council, Alternatives for Ground Water Cleanup, National Academy Press, Washington, DC, 1994.
[3] W. Kamolpornwijit, L. Liang, O.R. West, G.R. Moline, A.B. Sullivan, Preferential flow path development and its influence on long-term PRB performance: column study, J. Contam. Hydrol. 66 (2003) 161–178.
[4] N.E. Korte, Zero-valent Iron Permeable Reactive Barriers: A Review of Performance, Oak Ridge National Laboratory, Tennessee, 2001 (Environmental Sciences Division Publication No. 5056).
[5] L.A. Schipper, G.F. Barkle, J.C. Hadfield, M. Vojvodic-Vukovic, C.P. Burgess, Hydraulic constraints on the performance of a groundwater denitrification wall for nitrate removal from shallow groundwater, J. Contam. Hydrol. 69 (2004) 263–279.
[6] N. Gupta, T.C. Fox, Hydrogeologic modeling for permeable reactive barriers, J. Hazard. Mater. 68 (1999) 19–39.
[7] U.S. Environmental Protection Agency, Field Applications of In Situ Remediation Technologies: Permeable Reactive Barriers, Office of Solid Waste and Emergency Response, Technology Innovation Office, Washington, DC, 2002.
[8] U.S. Environmental Protection Agency, Permeable Reactive Barrier Technologies for Contaminant Remediation, Office of Solid Waste and Emergency Response, Washington, DC, 1998 (EPA/600/R-98/125).
[9] K.C. Scott, D.J. Folkes, Groundwater modeling of a permeable reactive barrier to enhance system performance, in: Proceedings of the 2000 Conference on Hazardous Waste Research, Denver, Colorado, May 23–25, 2000.
[10] C.M. Burger, P. Bayer, M. Finkel, Algorithmic funnel-and-gate system design optimization, Water Resour. Res. 43 (2007) 1–19, W08426.
[11] G.R. Eykholt, C.R. Elder, C.H. Benson, Effects of aquifer heterogeneity and reaction mechanism uncertainty on a reactive barrier, J. Hazard. Mater. 68 (1999) 73–96.
[12] P.S. Hemsi, C.D. Shackelford, An evaluation of the influence of aquifer heterogeneity on permeable reactive barrier design, Water Resour. Res. 42 (2006), W03402.
[13] N.-Z. Sun, W.W.-G. Yeh, Coupled inverse problems in groundwater modeling. 2. Identifiability and experimental design, Water Resour. Res. 26 (1990) 2527–2540.
[14] G. Christakos, B.R. Killam, Sampling design for classifying contaminant level using annealing search algorithms, Water Resour. Res. 29 (1993) 4063–4076.
[15] B.J. Wagner, Sampling design methods for groundwater modeling under uncertainty, Water Resour. Res. 31 (1995) 2581–2591.
[16] M.C. Hill, E.R. Banta, A.W. Harbaugh, E.R. Anderman, The U.S. Geological Survey modular ground-water model, user's guide to the observation, sensitivity, and parameter-estimation processes, U.S. Geological Survey, Open File Report 00-184, 2000.
[17] D.C. McKinney, D.P. Loucks, Network design for predicting groundwater contamination, Water Resour. Res. 28 (1992) 133–147.
[18] N.-Z. Sun, W.W.-G. Yeh, A stochastic inverse solution for transient groundwater flow: parameter identification and reliability analysis, Water Resour. Res. 28 (1992) 3269–3280.
[19] M.C. Hill, F.A. D'Agnese, C.C. Faunt, Guidelines for model calibration and application to simulation of flow in the Death Valley regional ground-water system, in: Proceedings of the 1999 ModelCARE Conference, Zurich, Switzerland, September, IAHS Publication 265, 1999, pp. 195–204.
[20] C.R. Tiedeman, M.C. Hill, F.A. D'Agnese, C.C. Faunt, Methods for using groundwater model predictions to guide hydrogeologic data collection, with application to the Death Valley regional groundwater flow system, Water Resour. Res. 39 (2003) (SBH-5-1-5-17).
[21] O.A. Cirpka, C.M. Burger, W. Nowak, M. Finkel, Uncertainty and data worth analysis for the hydraulic design of funnel-and-gate systems in heterogeneous aquifers, Water Resour. Res. (2004), W11502.
[22] J. Lee, Reliability-based approach to groundwater remediation design, Ph.D. Thesis, Northwestern University, IL, 2001.
[23] A.J. Graettinger, J. Lee, H.W. Reeves, D. Dethan, Quantitative methods to direct exploration based on hydrogeologic information, J. Hydroinform. 8 (2006) 77–90.
[24] J. Lee, H.W. Reeves, C.H. Dowding, The nodal failure index approach to groundwater remediation design, ASCE J. Geotech. Geoenviron. Eng., in press.
[25] A. Gelman, J.B. Carlin, H.S. Stern, D.B. Rubin, Bayesian Data Analysis, Chapman and Hall, London, United Kindom, 1995, pp. 478–479.
[26] A.J. Graettinger, C.H. Dowding, Directing exploration with 3-D FEM sensitivity and data uncertainty, ASCE J. Geotech. Geoenviron. Eng. 125 (1999) 959–967.
[27] C. Bischof, P. Khademi, A. Mauer, A. Carle, Adifor 2.0: automatic differentiating of fortran 77 programs, IEEE Comput. Sci. Eng. (1996) 18–32.
[28] M. Harr, Reliability-based Design in Civil Engineering, McGraw-Hill, New York, 1987.
[29] Department of Energy, Lower northeast area characterization and iron wall evaluation report, U.S. Department of Energy, Kansas City Area Office, Kansas City, MO, 2000.
[30] T. Supriyasilp, A.J. Graettinger, S.R. Durrans, Quantitatively directed sampling for main channel and hyporheic zone water quality modeling, Adv. Water Res. 26 (2003) 1029–1037.
[31] D. Dethan, Quantitatively directing exploration for hazardous waste site characterization using MODFLOW-2000, M.S. Thesis, University of Alabama, Tuscaloosa, AL, 2003.